IEEE Access
Multidisciplinary | Rapid Review | Open Access Journal

Received September 21, 2021, accepted September 30, 2021, date of publication October 4, 2021, date of current version October 12, 2021.

Digital Object Identifier 10.1109/ACCESS.2021.3117836

Restricted Access Window-Based Resource Allocation Scheme for Performance Enhancement of IEEE 802.11ah Multi-Rate IoT Networks

SRI PAVAN BADARLA, (Associate Member, IEEE), AND V. P. HARIGOVINDAN, (Senior Member, IEEE)

Department of Electronics and Communication Engineering, National Institute of Technology Puducherry, Karaikal, Puducherry 609609, India

Corresponding author: Sri Pavan Badarla (sripavan.rvce@gmail.com)

ABSTRACT IEEE 802.11ah (Wi-Fi HaLow) is introduced to support Internet of things (IoT) applications. In this paper, we consider the IEEE 802.11ah multi-rate IoT network where stations (STAs) contend for channel access using group-based restricted access window (RAW) mechanism with the default uniform grouping scheme. RAW divides the channel time into various slots, STAs into different groups and assigns a dedicated RAW slot to each group of STAs. As uniform grouping scheme performs grouping on random basis, each group will comprise of distinct data rate STAs, which leads to severe degradation of throughput because of performance anomaly. We propose a novel RAW based resource allocation (RAW-RA) scheme which groups the STAs in a multi-rate IoT network based on data rates and allocates the RAW slots to the groups proportional to their data rates. We also develop an accurate analytical model with unsaturated traffic conditions for calculating the throughput and energy efficiency of the IEEE 802.11ah multi-rate IoT network with the RAW mechanism. From the analytical results, it is evident that the proposed RAW-RA scheme can resolve the performance anomaly as well as significantly improves the aggregate throughput and energy efficiency of the IoT network. Finally, all the analytical results are validated with extensive simulation studies.

INDEX TERMS Internet of Things, IEEE 802.11ah, performance anomaly, restricted access window based resource allocation, Wi-Fi HaLow.

I. INTRODUCTION

The technological advancements in the networking field are evolving rapidly; as a consequence, stations (STAs) are able to access the Internet everywhere at high speed. This contributes to the rise in number of connected users to the Internet. The Internet of things (IoT) is a powerful paradigm in the modern world for interconnecting physical objects/things which are mostly energy constrained, for the applications such as smart grid, smart city, smart agriculture, smart home, and multimedia, etc. [1]. IoT enables objects with intelligence for sensing, computation, as well as information sharing through the Internet at anytime, anywhere, and for any service. The applications like e-Learning, e-Health, and smart environment lead to an increase in the number of connected users or STAs which make the network denser with challenging tasks [2].

Wireless local area networks (WLANs) have gained a lot of attention in recent years for providing Internet services compared to cellular networks. Despite WLANs are growing more popular in license-free bands, due to the widely deployed Wi-Fi access points (APs) for Internet access [3]. The IEEE 802.11 WLAN provides specifications for physical and medium access control (MAC) layers. The STAs at the physical layer of IEEE 802.11 WLAN exhibit multiple data rates over the AP's coverage area. The STAs closer to the AP attain higher signal strength and the STAs far from the AP exhibit poor signal strength depending on the distance from the AP. Thus, based on the signal-to-noise ratio (SNR), the STAs experience higher data rates when they are closer to the AP and lower data rates when they are far from the AP [4]. Using rate adaptation, the STAs can transmit the data

The associate editor coordinating the review of this manuscript and approving it for publication was Stefano Scanzio.

at various transmission rates to the AP. Besides, the MAC layer protocols play an important role in determining network performance. In the MAC layer, the STAs will contend using the fundamental channel access mechanism known as distributed coordination function (DCF) which works based on the carrier sense multiple access with collision avoidance (CSMA-CA). When STAs encounter collision, they undergo exponential back-off (BO) process [5]. Here, DCF guarantees equal channel access to all the STAs irrespective of their data rates to achieve fairness. Initially, Wi-Fi networks were designed for short distance communication with limited number of STAs for Internet access to ensure high throughput. Moreover, several traditional IEEE 802.11 standards operate around ISM bands of 2.4 GHz and 5 GHz which make the spectrum denser [6]. Therefore, the IEEE 802 working group introduced IEEE 802.11ah, as an amendment to the IEEE 802.11 to support dense IoT networks [7]. It features low power operation, massive number of STAs, and long transmission range.

A. BRIEF DISCUSSION ON IEEE 802.11ah STANDARD

IEEE 802.11ah standard is primarily developed for dense IoT networks. The standard operates in sub-1 GHz ISM bands which are unlicensed excluding the white space bands of television (TV). Therefore, a critical issue of the crowded spectrum that arises in other amendments of IEEE 802.11 WLAN could be minimized in IEEE 802.11ah [8]. In addition, the standard provides various enhancements to the physical and MAC layers, which are described as follows.

1) IEEE 802.11ah PHYSICAL LAYER CHARACTERISTICS

The physical layer of the IEEE 802.11ah standard is inherited from the IEEE 802.11ac and is ten times down-clocked to provide channel bandwidths of 2, 4, 8, and 16 MHz. Besides, 1 MHz channel is additionally introduced in IEEE 802.11ah for the extended range [7]. The standard exploits the orthogonal frequency division multiplexing (OFDM) technique at the physical layer. To support multiple data rates, the standard affords different modulation and coding schemes (MCSs) based on the channel conditions. Here, every STA can transmit at a particular data rate with the help of different MCSs (MCS0-MCS9) using rate adaptation. For extended coverage, MCS10 is introduced in 1 MHz channel with the BPSK modulation [9].

2) IEEE 802.11ah MAC LAYER CHARACTERISTICS

Several MAC layer enhancements are introduced in IEEE 802.11ah such as improved channel access mechanism, power-save (PS) methods, and scalability to support large number of STAs. To coordinate the large number of STAs, IEEE 802.11ah uses a hierarchical structure of association identifiers (AIDs), where the AP assigns a unique AID to every STA (typically 8192) [6]. In dense IoT networks, a high contention process is involved among the STAs for channel access. As a consequence, the network performance will be degraded. Hence, a group-based restricted access window (RAW) mechanism is introduced in the IEEE 802.11ah standard [7]. Here, a specified group of STAs are only permitted for medium access within the allocated time. The RAW mechanism of IEEE 802.11ah is shown in Fig. 1. In this, AP periodically transmits multiple beacon frames to every STA for network synchronization. In a beacon interval, there can be one or more RAW periods could be present. Under the RAW mechanism, the RAW period is divided into several RAW slots and the STAs are classified into various groups. Further, the RAW slots are assigned to the intended group of STAs. The group of STAs are allowed for channel access within the allocated RAW slot, which result in reduced collisions among the STAs. In this, the STAs can choose the deputed RAW slot using the expression $\phi_{slot} = (AID_n + F_{offset}) \mod K$, where AID_n is the n^{th} STA's AID, F_{offset} is for STA fairness, and K represents number of RAW slots [7]. Here, beacon frames carry RAW parameter set-information element (RPS-IE) to all the associated STAs which consists of RAW duration, each STA's AID, initial and end time of the corresponding RAW slot [10]. As shown in Fig. 1, the RAW slot is categorized into two parts. (1) Contention-based access period (2) holding period. The STAs identify the deputed RAW slot with the help of RPS-IE. Here, the RPS-IE consists of a cross slot boundary (CSB) field. If the CSB field is equal to zero, then the STAs should originate and finish their transmission within the RAW slot referred to as no-crossing case (NCR). Whereas, if the CSB field is set to one, the STAs can initiate the transmission within the RAW slot and can be permitted to continue their transmission after the boundary of the RAW slot known as crossing case [11].

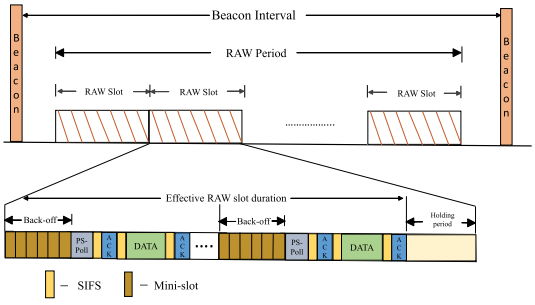

FIGURE 1. RAW mechanism of IEEE 802.11ah.

B. PERFORMANCE ANOMALY IN IEEE 802.11 MULTI-RATE NETWORKS

In IEEE 802.11 multi-rate networks, the STAs which are closer to the AP attain a higher rate due to the good channel conditions. These STAs use the minimum channel time for transmission of information once they acquire channel access. Despite, due to the poor channel conditions, the STAs at the fringes of the AP's coverage area exhibit lower data rates. To ensure fairness, IEEE 802.11 DCF guarantees equal opportunity for all the STAs in the network irrespective of their data rates [5]. As a result, the lower data rate STAs take longer transmission time once they acquire channel access.

Thus, the higher data rate STAs are unable to achieve high throughput because the medium is occupied by the lower data rate STAs for the majority of the time. Therefore, it penalizes the throughput performance of higher rate STAs and degrades the throughput down to that of lower rate STAs. This leads to performance anomaly in the network [12]. Earlier, IoT networks were designed for sending small data packets with infrequent transmissions. Nowadays, new emerging data-intensive IoT applications such as acoustic sensing, telepresence robots, wireless capsule endoscopy, and unmanned aerial vehicles require higher data rates. At present, the IoT scenario is a multi-rate scenario where different STAs has different data rate requirements [13]. In IEEE 802.11ah multi-rate network, the STAs contend for channel access using enhanced distributed channel access (EDCA) mechanism which is based on the DCF. Besides, the standard draft specifically does not mention any scheme for grouping. Hence, by default, a uniform grouping (UG) scheme is used [7]. UG scheme is a group-based scheme that randomly forms groups of equal size. In this paper, we propose a novel scheme to resolve the performance anomaly in IEEE 802.11ah multi-rate IoT networks because of the distinct data rate STAs present in the network, due to varying channel conditions.

The remaining portions of the paper are structured as follows: Section II presents the related research work. Section III describes the architecture of IEEE 802.11ah multi-rate IoT network and achievable data rate analysis. Section IV provides a detailed discussion of analytical model developed which is based on the discrete-time Markov-chain (DTMC) to evaluate the throughput and energy efficiency of the IEEE 802.11ah multi-rate IoT network. Section V shows the existence of performance anomaly in IEEE 802.11ah multi-rate IoT network. Section VI presents the proposed RAW based resource allocation (RAW-RA) scheme to resolve the anomaly and to improve the performance of the IEEE 802.11ah multi-rate IoT network. Section VII provides the analytical and simulation results. Section VIII describes conclusion.

II. RELATED WORK

The performance analysis of IEEE 802.11ah had been extensively studied in the literature [10], [11], [13]–[27]. In [10], [14], [15], the authors provided the various features of IEEE 802.11ah for different IoT scenarios. In [5], the author proposed a DTMC model to find the saturation throughput of IEEE 802.11 WLAN using DCF. After his pioneering work, several authors had extended the DTMC model for different versions of IEEE 802.11 WLAN supporting various applications. The authors of [11], [13], [16]–[27] evaluated the performance of IEEE 802.11ah network. A completely new approach referred to as mean value analysis was used by the authors of [11] for the throughput performance of IEEE 802.11ah network. Here, the average throughput, collision, and transmission probabilities were obtained by considering group-synchronized DCF (GS-DCF). The authors of [16] designed a smart metering network, in which they had suggested two grouping based MAC protocols that outperform the legacy DCF in dense networks. In their study, the authors modified the Markov-chain model by adding busy channel probability. In [13], the authors proposed a service differentiation scheme using GS-DCF to provide differentiated services. The authors in [17] proposed a model to improve the throughput of IEEE 802.11ah with the UG scheme. The authors of [18] presented a DTMC model for IEEE 802.11ah network to evaluate the average aggregate throughput with network simulations. In [19], the authors developed an analytical model based on a novel BO algorithm to compute the IEEE 802.11ah saturation throughput. The authors of [20] implemented an analytical model to improve the throughput of IEEE 802.11ah WLAN. In [21], the authors developed a mathematical model which is suitable for the IoT scenario according to the RAW mechanism. Here, the system performance was optimized by finding the optimal RAW parameters. The authors of [22] implemented a DTMC model with reset and renewal of BO to assess the performance of IEEE 802.11ah MAC layer for differentiated quality-of-service (QoS), without degrading the network performance. In [23], the authors proposed a QoS-aware priority grouping for real-time traffic conditions in IEEE 802.11ah network using a RAW scheduling scheme. It mitigates the collisions and provided the required bandwidth rare but priority to the critical traffic STAs.

As the IEEE 802.11ah standard promoted for low power applications, the authors of [24]–[27] evaluated the energy efficiency of the IEEE 802.11ah network. In [24], the authors proposed an optimal traffic sensor grouping scheme for the IEEE 802.11ah network. They developed a heuristic traffic sensor mapping algorithm to achieve sub-optimal energy efficiency with max-min fairness among groups. Using the DTMC model of [5], the authors in [25] provided a simple analytical model where the RAW mechanism gave better throughput and energy efficiency compared to legacy DCF. The authors of [26] proposed a novel medium access mechanism to mitigate the energy consumption in IEEE 802.11ah network. Here, it estimates the service interval and schedule the subsequent frames by eliminating the contention. In [27], the authors presented a novel directional MAC scheme using PS mechanism to improve the throughput and reduce the energy consumption for the IEEE 802.11ah network.

From the comprehensive survey of IEEE 802.11 multi-rate WLANs, a critical problem known as performance anomaly was identified in multi-rate networks that affects the throughput performance of high rate STAs [12]. Several studies were reported in the literature based on MAC parameters to mitigate the performance anomaly in IEEE 802.11 multi-rate WLANs [28]–[31]. The authors of [28] proposed a differentiated reservation algorithm to minimize the collisions and reduce the performance anomaly by sending multiple packets for one transmission opportunity. In [29], the authors used a proportional fairness approach to overcome the anomaly. The authors of [30] proposed a solution to anomaly by controlling the parameters such as frame size, initial and maximum

BO window. To resolve the anomaly, the authors in [31] proposed a MAC layer protocol for air-time fairness, where each STA runs numerous instances of conventional DCF BO process. Targeting IEEE 802.11ah multi-rate networks [32], [33], the authors of [32] proposed an analytical model where the STA after counting down to unity, checks for sufficient residual time for transmission of the frame and in case of insufficient residual time, STA enters the defer state. Also, the authors proposed a data rate grouping (DRG) scheme to solve the anomaly. In [33], the authors provided an analytical model for IEEE 802.11ah multi-rate network and proposed a novel grouping scheme to overcome the anomaly in dense networks.

In the RAW mechanism, each group of STAs assigned with a RAW slot. The STAs performing the BO decrement process in the assigned RAW slot, has to verify at each state for sufficient time to complete the frame transmission in the RAW slot [7]. If the residual time is insufficient, then the STAs will defer their attempt and wait for the next designated RAW slot by entering into a defer state. In such a case, the STAs must reset the BO counter and restart from the start of the next allocated RAW slot. The analytical models developed by the authors of [11], [13], [16]–[20], [23]–[27], [33] did not consider this important aspect of RAW mechanism, which is the reset and renewal of BO process at the beginning of RAW slot as per the IEEE 802.11ah standard [7]. Also, in [21] and [22], the authors proposed the analytical models for single-rate IEEE 802.11ah network; but neither of these two works provided a closed-form expression of throughput. In [32], the authors developed an analytical model which does not consider the checking of BO at each state in the DTMC model of the IEEE 802.11ah RAW mechanism. Hence, these models lack accuracy.

In this paper, differently from the previous works, we develop an accurate analytical model using DTMC analysis [5], [20], [22], [34] with unsaturated traffic conditions for IEEE 802.11ah, by considering the reset and renewal of BO counter at the RAW slot beginning as per the IEEE 802.11ah RAW mechanism [7]. The proposed model takes into account the reset of BO counter values at the end of the RAW slot irrespective of their BO stage. The model checks the residual time at each state and in case of insufficient residual time for a frame transmission, the STA enters into a defer state. After that, the STA will reset their BO counter values and renew them from the initial BO at the beginning of the next RAW slot. Thus the previous RAW slot counter values will not be carried to the next RAW slot according to the RAW mechanism. Hence, this model is accurate and completely in accordance with the IEEE 802.11ah standard [7]. The novel aspects of this research work are as follows.

(1) We develop an analytical model according to the IEEE 802.11ah RAW mechanism using DTMC analysis with unsaturated traffic conditions. Unlike the existing models, here residual time is checked at each state of the DTMC and STA enters into a defer state in case of insufficient residual time for frame transmission. This model is completely in conformance with IEEE 802.11ah standard and hence accurate.

(2) We propose a novel RAW-RA scheme to resolve the performance anomaly as well as to improve the aggregate utility and energy efficiency of the IEEE 802.11ah multi-rate IoT network with proportional resource allocation.

The contributions are described as follows.

- We develop an accurate analytical model where residual time is checked at each state of the DTMC with unsaturated traffic conditions to evaluate the throughput and energy efficiency of the IEEE 802.11ah multi-rate IoT network which uses DCF with RAW mechanism for medium sharing [5], [20], [22], [34]. This model takes into account the distinct features of the IEEE 802.11ah RAW mechanism in multi-rate IoT networks where the STAs communicate with different data rates.
- Using this model, we analyze the aggregate throughput of IEEE 802.11ah multi-rate IoT network with default UG scheme. From the results, we observe the significant degradation of throughput because of performance anomaly.
- We propose a novel RAW-RA scheme which groups the STAs in a multi-rate IoT network based on data rates and assigns RAW slots to the groups proportional to their data rates. We also analyze the performance of RAW-RA scheme using the analytical model developed with unsaturated traffic conditions. From the results, we observe that RAW-RA scheme can resolve the performance anomaly and significantly improves the aggregate throughput as well as energy efficiency of multi-rate IoT network compared to the DRG and default UG schemes. The proposed scheme can be implemented with lesser additional overhead because grouping is an imperative part of the IEEE 802.11ah RAW mechanism.
- We have conducted extensive simulation studies using network simulator (ns-3) which follows specifications of IEEE 802.11ah physical and MAC layers to corroborate the analytical findings.

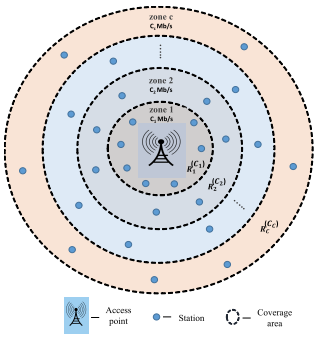

FIGURE 2. Network architecture with different zones. Zone 1, which is near to the AP consists of higher data rate STAs, while the zone *c* which is far from the AP comprises of lower data rate STAs.

III. NETWORK ARCHITECTURE

In this article, we consider an IEEE 802.11ah multi-rate IoT network with an AP at the center of the coverage area and

N number of STAs which are uniformly deployed around the AP as shown in Fig. 2. The STAs can communicate with the AP for uplink transmissions. At the IEEE 802.11ah physical layer, we consider c distinct data rates based on the average distance from the AP. The total coverage area of AP is divided into c zones with each of length w_x. Each STA is at a distance $R_x^{(C_x)}|x \in [1, c]$ from the AP. Hence, the supported data rates are $\Lambda_c = \{C_x|x \in [1, c]\}$. The zones are such that zone 1 is near the AP, whereas zone c is at the fringes of the AP. Further, the STAs near the AP exhibit a higher data rate, while the STAs at the fringes of the AP support lower data rate [4]. As the IEEE 802.11ah physical layer affords multiple data rates, each STA in a specific zone can transmit with the appropriate MCS using rate adaptation technique.

A. COMPUTATION OF ACHIEVABLE DATA RATE ANALYSIS

The analysis of achievable data rate is provided in this subsection for IEEE 802.11ah multi-rate network with macro deployment scenario [33], [35]. Here, the link budget for power received at the receiver STA of data rate $C_x|x \in [1, c]$ can be expressed as,

$$\mathcal{P}_r(R_x^{(C_x)}) = \mathcal{P}_t + A_t - L(R_x^{(C_x)}) + A_r, \tag{1}$$

where A_t denotes transmitter gain, A_r is receiver gain, $\mathcal{P}_t$ is transmitter power, and path loss $L(R_x^{(C_x)}) = 8 + 37.6\log_{10}(R_x^{(C_x)})$. The power loss component known as fade margin (F_M) exists in the network due to multipath fading. The power obtained in dB at the receiver STA of data rate $C_x|x \in [1, c]$ in zone-x considering Rayleigh-fading channel between the AP and STAs is given by,

$$\mathcal{P}_r(R_x^{(C_x)}) = \mathcal{P}_t + A_t - L(R_x^{(C_x)}) + A_r - F_M. \tag{2}$$

TABLE 1. Achievable data rates with zone lengths.

Zones	1	2	3	4	5
C_x (Mbps)	78	8.77	1.95	0.6	0.3
w_x (m)	115	210	307	420	505

The fade margin with respect to link outage is expressed as, $F_M = -10\log_{10}(-\ln(1 - P_{out}))$, where P_{out} is the outage probability. For the required level of link-outage $P_{out} = 0.1$ [35]. Furthermore, the SNR at the receiver STA is given by,

$$\frac{S}{N} = \frac{E_b}{N_0 B} \times \frac{1}{t_b} = \frac{C E_b}{k T_0 F B}, \tag{3}$$

where S is the power obtained at the receiver. According to Eq. (3), E_b represents energy consumed per bit, N_0 is the noise spectral density, t_b is bit duration, B is bandwidth, C is the data rate, k represents the Boltzmann constant, F is the noise figure, and receiver temperature in Kelvin is T_0. The Eq. (3) can be expressed in dB as,

$$\left(\frac{S}{N}\right)_{dB} = \left(\frac{E_b}{N_0}\right)_{dB} + \left(\frac{C}{B}\right)_{dB}. \tag{4}$$

From the Eq. (2) and Eq. (4), the achievable data rate of the receiver STA in zone-x is computed as,

$$C(R_x^{(C_x)}) = \mathcal{P}_t + A_t + A_r - L(R_x^{(C_x)}) - (N_0)_{dB} - F_M - \left(\frac{E_b}{N_0}\right)_{dB}. \tag{5}$$

The achievable data rates for the corresponding zone lengths are shown in Table 1.

IV. THROUGHPUT ANALYSIS OF IEEE 802.11ah MULTI-RATE IoT NETWORK

In this section, we develop an analytical model with unsaturated traffic conditions to determine the throughput and energy efficiency of the IEEE 802.11ah multi-rate IoT network, which uses DCF with RAW mechanism for medium sharing. We assume that no hidden STAs present in the network. From the network architecture discussed in Section III, the STAs are divided into c groups where the size of every group is n_x ($\sum_{x=1}^{c} n_x = N$). Here, we consider each group comprises an equal number of STAs and the STAs in each group are of the same data rate. Further, the RAW slots are formed by dividing the RAW period into various slots [11], with T_{RAW} representing the RAW period and $T_{s,k}$ gives the length of the k^{th} RAW slot. The duration of all the RAW slots is equal.

A. MARKOV-CHAIN MODEL

This subsection presents an accurate analytical model which is developed with unsaturated traffic conditions to evaluate the transmission probability of the x^{th} group STA of data rate $C_x|x \in [1, c]$ using DCF with the RAW mechanism [5], [20], [22], [34]. Here, the channel time is divided into mini-slots of duration σ_m. When the STA is ready to transmit a frame, it listens to the channel for distributed inter-frame space (DIFS) duration and contends for channel access by invoking the exponential BO procedure in the deputed RAW slot. During the BO, the STAs can select contention window (CW) in the range $[0, W_{k,0} - 1]$, where $W_{k,0}$ is the minimum CW. The two-dimensional Markov-chain model $\{a_k^{(C_x)}(t), b_k^{(C_x)}(t)\}$ is shown in Fig. 3 with a queue empty state I of probability $q_{0,k}$ which follows Poisson process with packet arrival rate of 100 packets/second [34]. Let the stochastic process of BO stage is $a_k^{(C_x)}(t)$, and $b_k^{(C_x)}(t)$ be the stochastic process corresponds to the BO counter that is evenly selected over the interval $[0, W_{k,0} - 1]$. Here, the discrete mini-slot times t and $t + 1$ represent the beginning of two consecutive BO of the STA. The duration of a mini-slot forms a random variable that could be an ideal/successful/collision slot. Let $p_{cn,k}^{(C_x)}$ is the probability of collision and $\tau_k^{(C_x)}$ is the transmission probability of the x^{th} group STA with data rate $C_x|x \in [1, c]$. These probabilities can be represented by Markov-chain model. Let the transmission duration of a frame for the STA with data rate $C_x|x \in [1, c]$ is given by,

$$T^{(C_x)} = T_{E[P]}^{(C_x)} + T_{SIFS} + T_{ack} + \sigma_p, \tag{6}$$

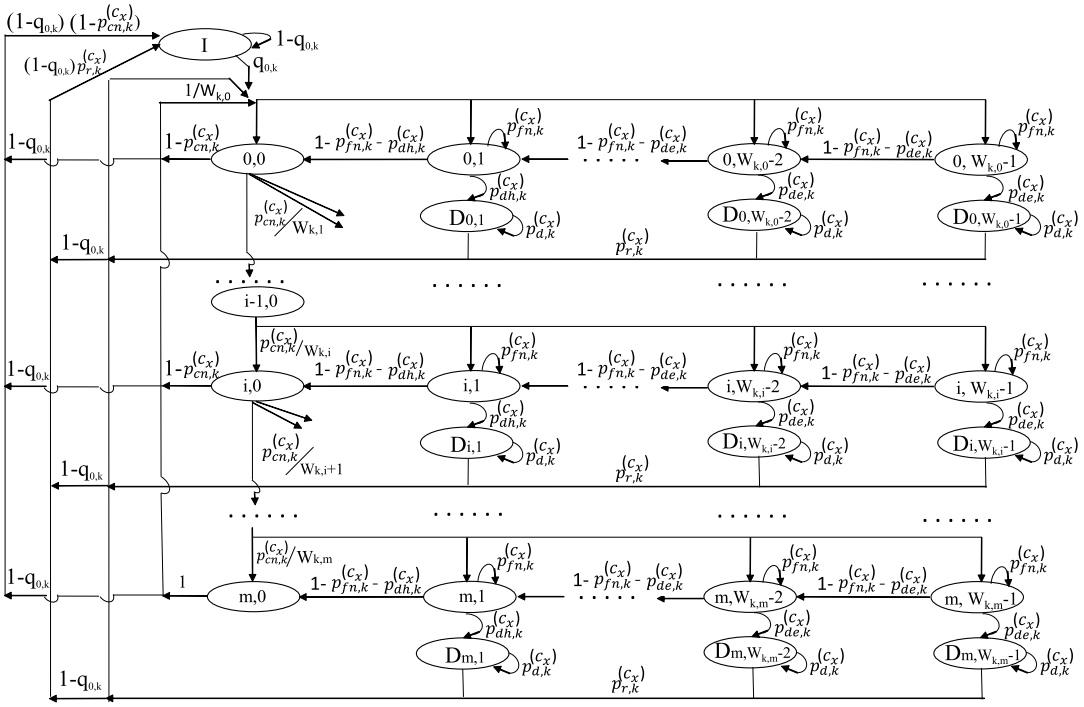

FIGURE 3. Markov-Chain model for IEEE 802.11ah RAW mechanism.

where payload duration is $T_{E[P]}^{(C_x)}$, T_{SIFS} represents the length of short IFS frame, T_{ack} is the acknowledgement (ACK) frame duration, and the propagation delay is σ_p. As shown in Fig. 1, AP specifies holding period at the end of every RAW slot for NCR case [11]. The holding period is given by $T_h = T^{(C_x)} - \sigma_m + \sigma_g$, where σ_g is guard band interval. Within the RAW slot, the initiation of any transmission should end before the holding period. As illustrated in Fig. 1, the effective RAW slot duration for contention is $T_{s',k} = T_{s,k} - T_h$. Here, the group of STAs access the channel in the deputed RAW slot using EDCA which is based on DCF. As the RAW slot is organized in contention-based access period and holding period, the total duration of RAW slot can be expressed as $T_{s,k} = T_{s',k} + T_h$. Here, the duration of a RAW slot is chosen such that, it must be at least as long as the transmission duration.

During the BO process, the STA decrements the BO counter in the deputed RAW slot when the channel is idle; otherwise, it freezes the counter. The x^{th} group STA's BO counter would be frozen due to the following aspects. (1) When the channel is sensed busy due to the transmission of another STA of the same group. (2) The contention-based access period of the deputed RAW slot is expired. Thus, the probability of BO counter will be frozen is given by,

$$p_{fn,k}^{(C_x)} = \frac{T_{s',k}}{T_{RAW}} \left(1 - (1 - \tau_k^{(C_x)})^{(n_k^{(C_x)}-1)}\right) \times \left(\prod_{p=1, p\neq x}^{c} (1 - \tau_k^{(C_p)})^{n_k^{(C_p)}}\right) + \frac{(T_{RAW} - T_{s',k})}{T_{RAW}}. \quad (7)$$

During the BO decrement process, at each state, the STA checks the residual time in the deputed RAW slot. When the residual time is not adequate for frame transmission during $j \in [2, W_{k,i} - 1]$, then the x^{th} group STA with data rate $C_x|x \in [1, c]$ enters into the deferred state is $p_{de,k}^{(C_x)}$. Here, the residual time is distributed evenly over the interval $(0, T_{s,k})$. The probability of x^{th} group STA with data rate $C_x|x \in [1, c]$ entering into deferred state is given by,

$$p_{de,k}^{(C_x)} = \begin{cases} \dfrac{T^{(C_x)}}{T_{s,k}}; & T^{(C_x)} \leq T_{s,k} \\ 1; & T^{(C_x)} > T_{s,k} \end{cases} \quad (8)$$

Similarly, when the BO counter reaches one, it decrements to zero, if the holding period in the deputed RAW slot is sufficient for the frame transmission. In case of the residual time is insufficient for successful frame transmission, then the STA moves into the deferred state as depicted in Fig. 3. Further, the STA will reset their BO functions and renew them from the initial BO for the next deputed RAW slot arrival. When the BO counter reaches one, let the probability of x^{th} group STA with data rate $C_x|x \in [1, c]$ entering into deferred state be $p_{dh,k}^{(C_x)}$. We assume that the residual time in the contention-based access period of the deputed RAW slot is distributed evenly over the interval $(0, T_{s',k})$ [32]. It is given by,

$$p_{dh,k}^{(C_x)} = \begin{cases} \dfrac{T^{(C_x)}}{T_{s',k}}; & T^{(C_x)} \leq T_{s',k} \\ 1; & T^{(C_x)} > T_{s',k} \end{cases} \quad (9)$$

The probability of x^{th} group STA transit from the deferred state be $p_{r,k}^{(C_x)} = \frac{T_{s,k}}{T_{RAW}}$, and the probability of STA being in the deferred state is $p_{d,k}^{(C_x)} = 1 - \frac{T_{s,k}}{T_{RAW}}$. Furthermore, a frame transmission occurs when the BO counter approaches zero irrespective of their BO stage. For every successful transmission, the STAs are being acknowledged with the ACK frame, and the BO counter reset to $W_{k,0}$. Whenever a packet collision occurs, the BO counter is doubled till the maximum CW. Here, we consider the maximum BO stage (m) is same as the retry limit.[1] Hence, the CW for i^{th} BO stage is given by $W_{k,i} = 2^i W_{k,0}, i \in [0, m]$. From the Markov-chain model, the probabilities corresponding to x^{th} group STA with data rate $C_x | x \in [1, c]$ can be expressed as,

$$P(i,j \mid i,j) = p_{fn,k}^{(C_x)}; \quad j \in [1, W_{k,i}-1],\ i \in [0,m] \tag{10a}$$

$$P(i,j-1 \mid i,j) = \begin{cases} 1-p_{fn,k}^{(C_x)}-p_{de,k}^{(C_x)}; & j \in [2, W_{k,i}-1] \\ 1-p_{fn,k}^{(C_x)}-p_{dh,k}^{(C_x)}; & j=1, i \in [0,m] \end{cases} \tag{10b}$$

$$P(i,j \mid i-1,0) = \frac{p_{cn,k}^{(C_x)}}{W_{k,i}}; \quad j \in [0, W_{k,i}-1],\ i \in [0,m] \tag{10c}$$

$$P(0,j \mid i,0) = \frac{(1-p_{cn,k}^{(C_x)})q_{0,k}}{W_{k,0}}; \quad j \in [0, W_{k,0}-1],\ i \in [0, m-1] \tag{10d}$$

$$P(0,j \mid m,0) = \frac{q_{0,k}}{W_{k,0}}; \quad j \in [0, W_{k,0}-1],\ i \in [0,m] \tag{10e}$$

$$P(I \mid i,0) = (1-q_{0,k})(1-p_{cn,k}^{(C_x)}); \quad i \in [0,m] \tag{10f}$$

$$P(D_{i,j} \mid D_{i,j}) = p_{d,k}^{(C_x)}; \quad j \in [1, W_{k,i}-1],\ i \in [0,m] \tag{10g}$$

$$P(D_{i,j} \mid i,j) = p_{de,k}^{(C_x)}; \quad j \in [2, W_{k,i}-1],\ i \in [0,m] \tag{10h}$$

$$P(D_{i,1} \mid i,1) = p_{dh,k}^{(C_x)}; \quad j=1,\ i \in [0,m] \tag{10i}$$

$$P(I/I) = (1-q_{0,k}); \tag{10j}$$

$$P(I \mid D_{i,j}) = p_{r,k}^{(C_x)}(1-q_{0,k}); \quad i \in [0,m] \tag{10k}$$

$$P(0,j \mid I) = \frac{q_{0,k}}{W_{k,0}}; \quad j \in [0, W_{k,0}-1] \tag{10l}$$

Here, Eq. (10a) represents the freezing probability of the x^{th} group STA when the channel is busy; Eq. (10b) signifies the probability of BO counter j decrements for $j \in [2, W_{k,i}-1]$ with probability $1 - p_{fn,k}^{(C_x)} - p_{de,k}^{(C_x)}$, while the BO counter reaches to zero by means of probability $1 - p_{fn,k}^{(C_x)} - p_{dh,k}^{(C_x)}$; Eq. (10c) represents the probability of STA entering the subsequent BO stage when it experiences collision; Eq. (10d) depicts the probability of STA reaches the BO stage zero when it successfully transmits, on a condition that the frame is ready in MAC layer buffer; Eq. (10e) accounts for the probability that, after the maximum number of transmission attempts, the STA moves into BO stage zero under the condition of MAC layer buffer nonempty; Eq. (10f) gives the probability of STA moves into queue empty state after the successful transmission when buffer is empty; Eq. (10g) represents the probability of STA remains in the deferred state; Eq. (10h) accounts for the probability of STA moves into the deferred state from the BO decrement state for $j \in [2, W_{k,i}-1], i \in [0,m]$; and Eq. (10i) signifies the probability of STA moves into the deferred state from the BO decrement state for $j = 1, i \in [0,m]$; Eq. (10j) gives the probability of STA being in the queue empty state; Eq. (10k) represents the probability of STA moves to queue empty state from the deferred state when the MAC layer buffer is empty; Eq. (10l) accounts for the probability of STA moves into initial BO stage when the MAC layer buffer is ready with a frame.

[1]Here, the number of BO stages $m = 7$ is the retry limit and minimum CW=32.

Stationary distribution of the Markov-chain model corresponds to the x^{th} group STA with data rate $C_x | x \in [1, c]$ is given by,

$$b_k^{(C_x)}(i,j) = \lim_{t\to\infty} P\{a_k^{(C_x)}(t) = i, b_k^{(C_x)}(t) = j\}; \quad j \in [0, W_{k,i}-1], \quad i \in [0,m] \tag{11}$$

Under steady-state conditions, the following relations obtained by solving the Markov-chain model.

$$b_k^{(C_x)}(i,0) = (p_{cn,k}^{(C_x)})^i b_k^{(C_x)}(0,0); \quad i \in [0,m] \tag{12}$$

$$b_k^{(C_x)}(i,j) = \frac{W_{k,i}-j}{W_{k,i}} \frac{(p_{cn,k}^{(C_x)})^i b_k^{(C_x)}(0,0)}{1-p_{fn,k}^{(C_x)}-p_{de,k}^{(C_x)}}; \quad j \in [2, W_{k,i}-1],\ i \in [1,m] \tag{13}$$

$$b_k^{(C_x)}(i,1) = \frac{W_{k,i}-1}{W_{k,i}} \frac{(p_{cn,k}^{(C_x)})^i b_k^{(C_x)}(0,0)}{1-p_{fn,k}^{(C_x)}-p_{dh,k}^{(C_x)}}; \ i \in [1,m] \tag{14}$$

$$b_k^{(C_x)}(D_{i,j}) = \frac{W_{k,i}-j}{W_{k,i}} \frac{(p_{cn,k}^{(C_x)})^i b_k(0,0)}{1-p_{fn,k}^{(C_x)}-p_{de,k}^{(C_x)}} \left(\frac{p_{de,k}^{(C_x)}}{p_{r,k}^{(C_x)}}\right); \quad j \in [2, W_{k,i}-1],\ i \in [0,m] \tag{15}$$

$$b_k^{(C_x)}(D_{i,1}) = \frac{W_{k,i}-1}{W_{k,i}} \frac{(p_{cn,k}^{(C_x)})^i b_k^{(C_x)}(0,0)}{1-p_{fn,k}^{(C_x)}-p_{dh,k}^{(C_x)}} \left(\frac{p_{dh,k}^{(C_x)}}{p_{r,k}^{(C_x)}}\right); \quad j=1,\ i \in [0,m] \tag{16}$$

$$b_k^{(C_x)}(0,j) = \frac{W_{k,i}-j}{1-p_{fn,k}^{(C_x)}-p_{de,k}^{(C_x)}} \times G; \quad j \in [2, W_{k,i}-1], \tag{17}$$

$$b_k^{(C_x)}(0,1) = \frac{W_{k,i}-1}{1-p_{fn,k}^{(C_x)}-p_{dh,k}^{(C_x)}} \times G; \quad j=1 \tag{18}$$

where

$$G = \left(\begin{array}{c} \frac{q_{0,k}(1-p_{cn,k}^{(C_x)})}{W_{k,0}} \sum_{i=0}^{m-1} b_k^{(C_x)}(i,0) + \frac{q_{0,k}}{W_{k,0}} b_k^{(C_x)}(m,0) \\ + \frac{p_{de,k}q_{0,k}}{W_{k,0}} \sum_{i=0}^{m} \sum_{j=2}^{W_{k,i}-1} b_k^{(C_x)}(i,j) \\ + \frac{p_{dh,k}q_{0,k}}{W_{k,0}} \sum_{i=0}^{m} b_k^{(C_x)}(i,1) + \frac{q_{0,k}}{W_{k,0}} b_k(I) \end{array} \right).$$

Under the steady-state probabilities, the normalized condition is given by,

$$\sum_{i=0}^{m}\sum_{j=2}^{W_{k,i}-1} b_k^{(C_x)}(i,j)+\sum_{i=0}^{m} b_k^{(C_x)}(i,1)+\sum_{i=0}^{m} b_k^{(C_x)}(i,0) +\sum_{i=0}^{m}\sum_{j=2}^{W_{k,i}-1} b_k^{(C_x)}(D_{i,j})+\sum_{i=0}^{m} b_k^{(C_x)}(D_{i,1})+b_k(I)=1 \quad (19)$$

After substituting and simplifying the equations from (12) to (18) in the Eq. (19), the expression for $b_k^{(C_x)}(0,0)$ is given by,

$$b_k^{(C_x)}(0,0)=\frac{1}{\left(\begin{array}{c}1+Y_1+Y_2+Y_3+Y_4+\frac{1-q_{0,k}}{q_{0,k}}+\\ (Y_5+Y_6)(\alpha+\beta+\frac{1-q_{0,k}}{q_{0,k}})\end{array}\right)}, \quad (20)$$

where

$$Y_1=\frac{\alpha\, p_{cn,k}^{(C_x)}(1-(2p_{cn,k}^{(C_x)})^m)W_{k,0}}{1-2p_{cn,k}^{(C_x)}}$$

$$Y_2=\frac{p_{cn,k}^{(C_x)}(1-(p_{cn,k}^{(C_x)})^m)(1-1.5\alpha+\beta)}{1-p_{cn,k}^{(C_x)}}$$

$$Y_3=\frac{p_{cn,k}^{(C_x)}(2^m-(p_{cn,k}^{(C_x)})^m)(\alpha-\beta)}{2^m(2-p_{cn,k}^{(C_x)})W_{k,0}}$$

$$Y_4=\frac{((W_{k,0})^2-3W_{k,0}+2)(\alpha+2\beta)}{W_{k,0}}$$

$$Y_5=\frac{0.5\gamma\,(1-(2p_{cn,k}^{(C_x)})^{m+1})}{(1-2p_{cn,k}^{(C_x)})}-\frac{(1-(p_{cn,k}^{(C_x)})^{m+1})(1.5\gamma-\eta)}{(1-p_{cn,k}^{(C_x)})W_{k,0}}$$

$$Y_6=\frac{(2^{m+1}-(p_{cn,k}^{(C_x)})^{m+1})(\gamma-\eta)}{2^m(W_{k,0})^2(2-p_{cn,k}^{(C_x)})}$$

also, $\alpha=\frac{1+(p_{de,k}^{(C_x)}/p_{r,k}^{(C_x)})}{1-p_{fn,k}^{(C_x)}-p_{de,k}^{(C_x)}}$, $\beta=\frac{1+(p_{dh,k}^{(C_x)}/p_{r,k}^{(C_x)})}{1-p_{fn,k}^{(C_x)}-p_{dh,k}^{(C_x)}}$, $\gamma=\frac{p_{de,k}^{(C_x)}}{1-p_{fn,k}^{(C_x)}-p_{de,k}^{(C_x)}}$, and $\eta=\frac{p_{dh,k}^{(C_x)}}{1-p_{fn,k}^{(C_x)}-p_{dh,k}^{(C_x)}}$.

The transmission probability of the x^{th} group STA with data rate $C_x|x\in[1,c]$ in the mini-slot of the deputed k^{th} RAW slot can be computed as,

$$\tau_k^{(C_x)}=\sum_{i=0}^{m} b_k^{(C_x)}(i,0)=\frac{1-(p_{cn,k}^{(C_x)})^{m+1}}{1-p_{cn,k}^{(C_x)}}b_k^{(C_x)}(0,0). \quad (21)$$

The probability of the x^{th} group STA with data rate $C_x|x\in[1,c]$ which suffers from the collision in the mini-slot of the deputed k^{th} RAW slot is expressed as,

$$p_{cn,k}^{(C_x)}=(1-(1-\tau_k^{(C_x)})^{n_k^{(C_x)}-1}) \times\prod_{p=1,p\neq x}^{c}(1-\tau_k^{(C_p)})^{n_k^{(C_p)}}(1-e_r), \quad (22)$$

where packet error rate $e_r=0.1$. The probability that the x^{th} group STA with data rate $C_x|x\in[1,c]$ succeeds its transmission in the mini-slot of the deputed k^{th} RAW slot is given by,

$$p_{s,k}^{(C_x)}=\frac{1}{p_{tr,k}^{(C_x)}}\times\left(n_k^{(C_x)}\tau_k^{(C_x)}(1-\tau_k^{(C_x)})^{n_k^{(C_x)}-1}\right) \times\left(\prod_{p=1,p\neq x}^{c}(1-\tau_k^{(C_p)})^{n_k^{(C_p)}}(1-e_r)\right), \quad (23)$$

where the probability of at least one STA transmits with data rate $C_x|x\in[1,c]$ in the mini-slot of the deputed k^{th} RAW slot is expressed as,

$$p_{tr,k}^{(C_x)}=1-\prod_{p=1}^{c}(1-\tau_k^{(C_p)})^{n_k^{(C_p)}}. \quad (24)$$

The sum of a $T^{(C_x)}$, T_{DIFS}, and the number of BO slots spent prior to the transmission would account for a transaction. Let $\lambda_{b,\omega}$ implies the number of mini-slots spent before the ω^{th} transmission and δ_ω is the length of ω-transactions. Thus, the probability of δ_ω in the deputed RAW slot that utilizes the λ mini-slots [11] is expressed as,

$$\mathbb{P}_{\delta_\omega}(\lambda)=\binom{\lambda-\omega T^{'}-1}{\lambda-\omega T^{'}-\omega}(p_{tr,k}^{(C_x)})^{\omega}(1-p_{tr,k}^{(C_x)})^{\lambda-\omega T^{'}-\omega}, \quad (25)$$

where $T^{'}=T^{(C_x)}+T_{DIFS}$. Let the random variable $\mathcal{H}$ be the total number of transactions during $T_{s',k}$. The probability of ω-transactions in the deputed k^{th} RAW slot can be expressed as,

$$\mathbb{P}_{\mathcal{H},k}(\omega)=\sum_{x=\omega}^{T_{s',k}-(\omega-1)T^{'}-T_{DIFS}-\sigma_m} Prob\left\{\sum_{k=1}^{\omega}\lambda_{b,k}=x\right\}. \quad (26)$$

The maximum number of transmissions during $T_{s',k}$ can be expressed as $\mathcal{N}_T=\lfloor\frac{T_{s',k}}{T^{'}+\sigma_m}\rfloor$. Therefore, the average value of $\mathcal{H}$ during the deputed k^{th} RAW slot can be expressed as,

$$\mathbb{E}_k[\mathcal{H}]=\sum_{\omega=1}^{\mathcal{N}_T(T_{s,k}-T_h)}\omega\mathbb{P}_{\mathcal{H},k}(\omega). \quad (27)$$

Therefore, the average throughput of the x^{th} group STA with data rate $C_x|x\in[1,c]$ in the deputed k^{th} RAW slot is given by,

$$UT_k^{(C_x)}=\frac{c\,E[P]\,\mathbb{E}_k[\mathcal{H}]\,p_{s,k}^{(C_x)}}{T_{RAW}}. \quad (28)$$

By considering the UG scheme, the aggregate throughput of a group having distinct data rate STAs of data rate $C_x|x\in[1,c]$ in the deputed k^{th} RAW slot is given by,

$$UT_k=\sum_{x=1}^{c}UT_k^{(C_x)}. \quad (29)$$

The data transferred by the x^{th} group STA with data rate $C_x|x \in [1, c]$ can be computed as,

$$D_k^{(C_x)} = \frac{c\, E[P]\, \mathbb{E}_k[\mathcal{H}]\, p_{s,k}^{(C_x)}}{T_{RAW}} \left(T_{s',k} + T_h\right). \quad (30)$$

B. ENERGY EFFICIENCY ANALYSIS

The energy efficiency is the amount of energy required to successfully transmit the data bits [36], [37]. During the DCF mechanism, the STA can be in one of the following states such as decrementation, freezing of BO counter, successful transmission or collision. The STA with data rate $C_x|x \in [1, c]$ that can consume energy in the BO procedure is $\mathbb{E}_{B,k}^{(C_x)}$, freezing state is $\mathbb{E}_{F,k}^{(C_x)}$, successful transmission is $\mathbb{E}_{s,k}^{(C_x)}$, and the collision process is $\mathbb{E}_{cn,k}^{(C_x)}$. Hence, the energy efficiency can be expressed as,

$$\mathbb{E}_T^{(C_x)} = \frac{\mathbb{E}_{B,k}^{(C_x)} + \mathbb{E}_{F,k}^{(C_x)} + \mathbb{E}_{s,k}^{(C_x)} + \mathbb{E}_{cn,k}^{(C_x)}}{E[P]}. \quad (31)$$

During the BO counter decremented process, the energy consumed is given by,

$$\mathbb{E}_{B,k}^{(C_x)} = \sum_{r=0}^{m} (1 - p_{cn,k}^{(C_x)})(p_{cn,k}^{(C_x)})^r \sum_{u=0}^{r} \frac{W_{k,u} - 1}{2} \sigma_m \mathcal{P}_{id}, \quad (32)$$

here $\mathcal{P}_{id}$ is the idle power. In the deputed RAW slot, the probability of one of the $(n_k^{(C_x)} - 1)$ STAs transmit successfully can be expressed as,

$$p_{s',k}^{(C_x)} = \frac{(n_k^{(C_x)} - 1)\tau_k^{(C_x)}(1 - \tau_k^{(C_x)})^{(n_k^{(C_x)} - 2)}}{1 - (1 - \tau_k^{(C_x)})^{(n_k^{(C_x)} - 1)}}. \quad (33)$$

In the BO process, the number of times that the transmissions overhear by the other STAs is given by,

$$\mathcal{Q} = \frac{p_{cn,k}^{(C_x)} \sum_{r=0}^{m} (1 - p_{cn,k}^{(C_x)})(p_{cn,k}^{(C_x)})^r \sum_{u=0}^{r} \frac{W_{k,u} - 1}{2}}{1 - p_{cn,k}^{(C_x)}}. \quad (34)$$

The energy consumed by a STA in the BO process due to overhear from the other STAs is expressed as,

$$\mathbb{E}_{F,k}^{(C_x)} = \mathcal{Q}[\Delta_{cn}(1 - p_{s',k}^{(C_x)}) + \sigma_m p_{s',k}^{(C_x)}]\mathcal{P}_{id}, \quad (35)$$

where $\Delta_{cn} = T_{poll} + T_{DIFS} + \sigma_p$ is duration of collision process. Here, T_{poll} is PS-Poll frame duration. The energy consumed during the successful transmission is given by,

$$\mathbb{E}_{s,k}^{(C_x)} = (T_{poll} + T_{E[P]}^{(C_x)})\mathcal{P}_t + (\Delta_s - T_{poll} - T_{E[P]}^{(C_x)})\mathcal{P}_r, \quad (36)$$

where successful transmission duration $\Delta_s = T_{poll} + T_{E[P]}^{(C_x)} + 2T_{ack} + 3T_{SIFS} + T_{DIFS} + 3\sigma_p$. The average number of transmission attempts due to the collisions prior to the success can be computed as,

$$\mathcal{Q}_{cn} = \sum_{r=0}^{m} r(1 - p_{cn,k}^{(C_x)})(p_{cn,k}^{(C_x)})^r. \quad (37)$$

The energy consumed because of the collision process is given by,

$$\mathbb{E}_{cn,k}^{(C_x)} = \mathcal{Q}_{cn}[(T_{poll})\mathcal{P}_t + (T_{DIFS} + \sigma_p)\mathcal{P}_r]. \quad (38)$$

Using the equations from (32), (35), (36), and (38), the energy efficiency of the network can be computed based on Eq. (31).

V. PERFORMANCE ANOMALY IN IEEE 802.11ah MULTI-RATE IoT NETWORK

In this section, we consider an AP whose coverage area is classified into five different zones. The zones are positioned in such a way that, zone 5 is at the fringes of the AP having STAs of lowest data rate. While, zone 1 is closer to the AP with the STAs of highest data rate as depicted in Table 1 of Section III. To observe the existence of performance anomaly, we have examined two cases. In the case-1, we consider the UG scheme of group size $n_x = 200$ which comprises of 40 distinct data rate STAs from each of the five zones. Further, we have computed the aggregate throughput using Eq. (29). In case-2, we consider the STAs with a group size of $n_x = 200$ of lowest data rate alone (0.3 Mbps), and we compute the throughput using Eq. (28). The results of case-1 and case-2 have been tabulated in Table 2. From Table 2, we have observed the throughput of the group of distinct data rate STAs (case-1) is degraded close to the lowest data rate group STAs (case-2). This is because of performance anomaly. Since all the distinct data rate STAs in the UG scheme have an equal chance of accessing the channel, which result in lowest data rate STAs use the channel most of the time. This penalizes the channel time of highest rate STAs and the throughput performance degrades because of inappropriate usage of channel resources.

TABLE 2. Throughput for case-1 and case-2.

	Analytical (Kbps)	Simulation (Kbps)
Case-1	0.1945	0.2189
Case-2	0.1065	0.1106

VI. RESOLVING PERFORMANCE ANOMALY AND RESOURCE ALLOCATION: RAW-RA SCHEME

In this section, we propose a RAW-RA scheme to resolve the performance anomaly as well as to improve the aggregate utility of the IEEE 802.11ah multi-rate IoT network. The proposed scheme groups the STAs based on the data rates and allows them to contend in the deputed RAW slot. As illustrated in Algorithm 1, the proposed RAW-RA scheme is described as follows. Initially, at regular intervals, AP transmits multiple beacons to every STA in the network. After hearing the beacon frame, every STA computes its data rate as stated in Table 1 of Section III before the association process. The achievable data rate of each STA is shared with the AP through the rate bits of the physical layer convergence protocol (PLCP) header during the association process. The AP then classifies the STAs based on data rates and form a RAW-RA matrix. Every row in the RAW-RA matrix represent a group of the same data rate STAs which are formed into c groups, and every STA is assigned with a unique AID by

Algorithm 1 Proposed RAW-RA Scheme

Each STA initially share its achievable data rate with the AP;
A RAW-RA matrix is formed and initialized as null matrix;
$p \leftarrow 1,\ q \leftarrow 1$;
while $p \leq \Lambda_c$ **do**
  while $q \leq N$ **do**
    if n_q transmits with data rate $C_x | x \in [1, c]$ **then**
      $M[p][q] \leftarrow n_q$;
    end if
    $q \leftarrow q + 1$
  end while
  $p \leftarrow p + 1$
end while
$p \leftarrow 1,\ q \leftarrow 1$;
while $p \leq \Lambda_c$ **do**
  while $q \leq N$ **do**
    Each RAW-RA matrix's row is formed as a group by the AP based on the same data rates and assigns a group ID to each group;
    $q \leftarrow q + 1$
  end while
  $p \leftarrow p + 1$
end while/* **Slot allocation procedure***/
$u \leftarrow 1$;
while $u \leq \Lambda_c$ **do**
  $\phi_{Slot-initial} \leftarrow (AID_n + F_{offset}) \mod K$;
  $Slot\_num \leftarrow \phi_{Slot-initial}$;
  $y \leftarrow c$; /* Temporary variable */
  $z \leftarrow G_{id}$;
  while $z < c$ **do**
    $Slot\_num \leftarrow Slot\_num + y$;
    $y \leftarrow (y - 1)$;
    $A[Slot\_num] \leftarrow Slot\_num$;
    $z \leftarrow z + 1$
  end while
  $u \leftarrow u + 1$
end while
STAs in the respective group can choose any RAW slot of $A[Slot\_num]$ & $\phi_{Slot-initial}$;

the AP. Here, the LSB bits of all STAs belong to a group are the same. Therefore, AP can assign a group ID (G_{id}) to each group. Using RPS-IE, the details of assigned AIDs, RAW initial, end time, and the number of groups are shared with the STAs.

TABLE 3. RAW slots allocation based on data rates.

Data rate (Mbps)	Group ID (G_{id})	Number of slots	Slots assigned
78	0	5	0,5,9,12,14
8.77	1	4	1,6,10,13
1.95	2	3	2,7,11
0.6	3	2	3,8
0.3	4	1	4

Furthermore, we allocate the channel resources to every group proportional to their data rates. We consider the entire RAW duration has 15 RAW slots numbered from RAW slot 0 to RAW slot 14. The slot allocation procedure is provided in Algorithm 1. Based on the slot allocation procedure, the STAs in the group 1, which has the highest data rate can choose the RAW slots of 0, 5, 9, 12, and 14 as shown in Table. 3. Similarly, the STAs in the group 5 of lowest data rate can only choose the RAW slot 4. As shown in Table. 3, the throughput of the group of same data rate STAs is computed based on the number of RAW slots assigned using the RAW-RA scheme. Here, the proposed scheme can be implemented very easily without any significant modifications to the existing standard, because grouping is an imperative part of the RAW mechanism in IEEE 802.11ah.

VII. RESULTS AND DISCUSSION

This section presents analytical results that are validated with extensive simulation studies. Simulations are performed using ns-3.29 [38]. We consider an IEEE 802.11ah multi-rate IoT network with uniformly deployed 1000 number of STAs in the AP's coverage area as shown in Fig. 2. The AP's coverage area is divided into five different zones corresponding to the data rates as provided in Table 1. The zone 1, which is near to the AP has highest data rate STAs, while the zone 5 which is at the fringes of the AP has lowest data rate STAs. The simulations are conducted for 100 seconds, 30 times with a confidence interval of 95% and averaged to evaluate the throughput. We have selected the system parameters based on the IEEE 802.11ah standard. The system parameters are provided in Table 4.

TABLE 4. System parameters.

Parameter	Value
Payload, $E[P]$	64 bytes
MAC header	14 bytes
Physical header	156 bits
ACK	112 bits
T_{DIFS}	264 μs
T_{SIFS}	160 μs
σ_m	52 μs
σ_p	1 μs
T_{RAW}	500 ms
PS-Poll frame	20 bytes
Idle power, $\mathcal{P}_{id}$	1 μW
Fade margin, F_M	9.77 dB
Noise figure, F	2
Transmitter gain, A_t	3 dB
Receiver gain, A_r	0 dB
Coverage	1000 m
Propagation model	Outdoor, Macro
Number of stations	1000
Simulation time	100 s
RAW groups	5

Figure 4 shows the throughput performance of the proposed RAW-RA scheme compared to the DRG scheme [32] and default UG scheme. In the RAW-RA scheme, all the STAs are divided into five groups based on the data rates using Algorithm 1. Here, we provide more number of RAW slots to high rate STAs. To illustrate this, the total RAW duration is divided into 15 RAW slots, and the RAW slots are allocated proportional to their data rates as provided in Table. 3. Here, group 1 (zone 1) comprises of highest data rate STAs assigned with five RAW slots, whereas group 5 (zone 5) consists of lowest data rate STAs allocated with one RAW slot. Similarly,

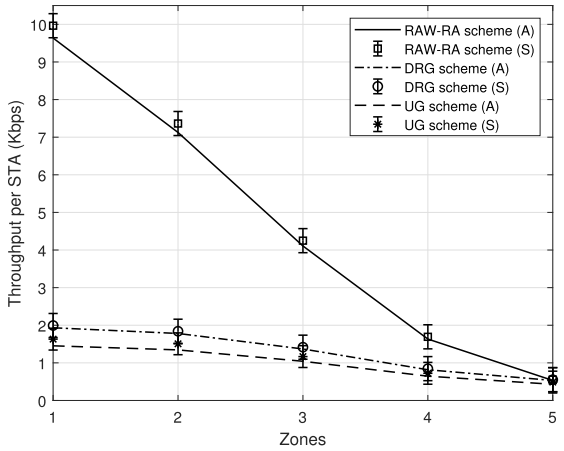

FIGURE 4. Throughput per station versus different zones.

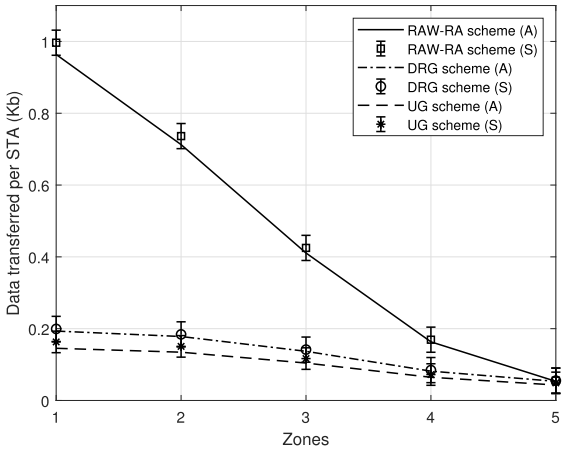

FIGURE 6. Data transferred per station versus different zones.

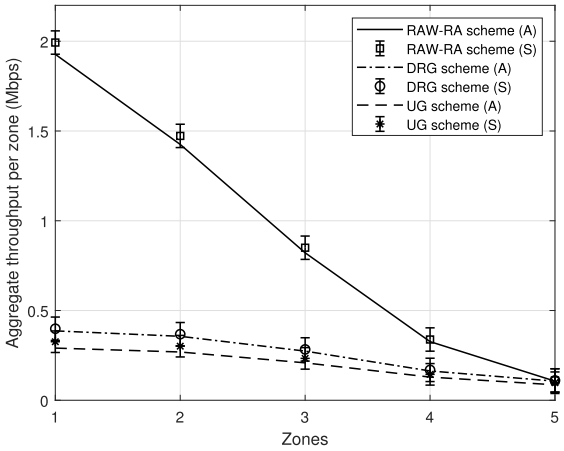

FIGURE 5. Aggregate throughput per zone versus different zones.

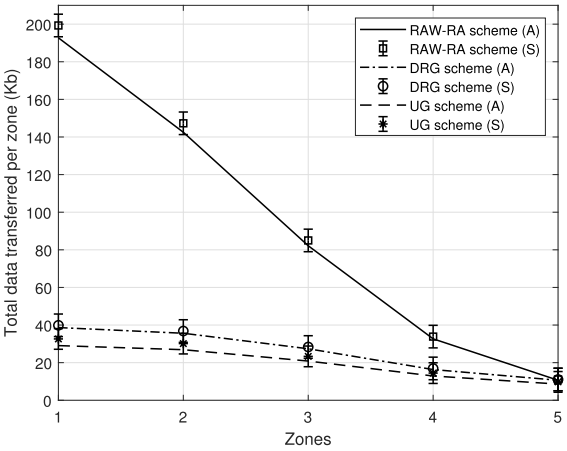

FIGURE 7. Total data transferred per zone versus different zones.

in the UG scheme, the network is classified into five different groups with an equal number of distinct data rate STAs from each of the five zones. In the UG scheme, the slot allocation procedure is uniform as it gives equal chance to every STA irrespective of their data rates. Hence, we provide every group with one RAW slot of duration 100 ms. From Fig. 4, it is evident that the proposed RAW-RA scheme resolves the performance anomaly and significantly improves the throughput performance of the IEEE 802.11ah multi-rate IoT network. In addition, we also compute the aggregate throughput per zone. Figure 5 gives the aggregate throughput per zone for the RAW-RA, DRG, and UG schemes. The findings show that a significant improvement in the aggregate throughput per zone can be observed with the proposed RAW-RA scheme compared to the DRG and UG schemes.

Figure 6 shows the data transferred (Kb) per STA for the IEEE 802.11ah multi-rate IoT network. The data transferred per STA is computed using Eq. (30). After grouping the STAs based on their data rates, the proposed RAW-RA scheme allocates more channel resources to higher rate STAs (zone 1) than lower rate STAs (zone 5). From Fig. 6, we can observe that the data transferred per STA is considerably improved compared to DRG and UG schemes. Figure 7 shows the total data transferred (Kb) per zone for IEEE 802.11ah multi-rate IoT network. From Fig. 7, we can observe the proposed RAW-RA scheme substantially improves the total data transferred per zone over the DRG and UG schemes.

Figure 8 shows the energy efficiency analysis with respect to the zones. From Fig. 8, we can observe less energy consumption using the proposed scheme when compared to the DRG and UG schemes. This is due to the STAs which are far from the AP have lower data rates. Thus, these STAs utilize the channel for longer time and consume more energy. While, the STAs near the AP has a higher data rate, eventually these STAs use minimum channel time for transmission and consume less energy. The energy efficiency is significantly better in the proposed scheme when compared to the DRG and UG schemes. By examining all the results, it is evident that the proposed RAW-RA scheme outperforms the DRG and UG schemes in terms of throughput performance and energy efficiency of the IEEE 802.11ah multi-rate IoT network.

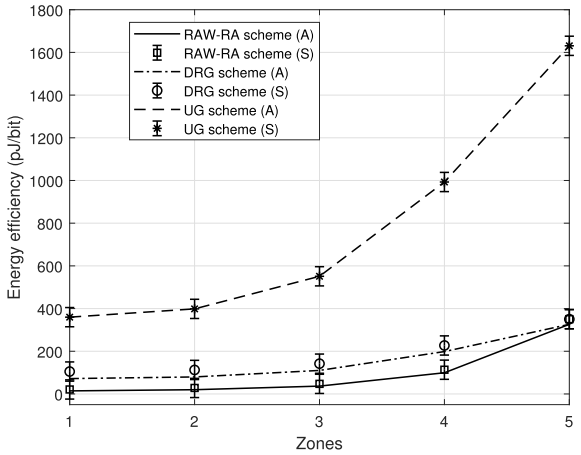

FIGURE 8. Energy efficiency versus different zones.

VIII. CONCLUSION

In this paper, we have developed an accurate analytical model with unsaturated traffic conditions to compute the throughput and energy efficiency of the IEEE 802.11ah multi-rate IoT network under the RAW mechanism, considering the STAs operate at distinct data rates. We have evaluated the aggregate throughput using the default UG scheme and observed that the throughput has been degraded greatly because of performance anomaly. This is due to the inappropriate usage of channel resources by the lower rate STAs. Hence, we have proposed a novel RAW based resource allocation (RAW-RA) scheme for the IEEE 802.11ah multi-rate IoT network. With the proposed scheme, the STAs in a multi-rate IoT network are grouped based on the data rates and the RAW slots are allocated to each group proportional to their data rates. It is observed that the proposed RAW-RA scheme can simultaneously resolve the performance anomaly and improved the aggregate throughput as well as energy efficiency of the IEEE 802.11ah multi-rate IoT network when compared to the DRG and UG schemes. We have used the network simulator (ns-3) which follows IEEE 802.11ah physical and MAC layer specifications to validate the analytical results.

REFERENCES

[1] A. Nauman, Y. A. Qadri, M. Amjad, Y. B. Zikria, M. K. Afzal, and S. W. Kim, "Multimedia Internet of Things: A comprehensive survey," *IEEE Access*, vol. 8, pp. 8202–8250, 2020.

[2] V. Baños-Gonzalez, M. Afaqui, E. Lopez-Aguilera, and E. Garcia-Villegas, "IEEE 802.11ah: A technology to face the IoT challenge," *Sensors*, vol. 16, no. 11, p. 1960, Nov. 2016.

[3] B. Bellalta, L. Bononi, R. Bruno, and A. Kassler, "Next generation IEEE 802.11 wireless local area networks: Current status, future directions and open challenges," *Comp. Commun.*, vol. 75, pp. 1–25, Feb. 2016.

[4] V. P. Harigovindan, A. V. Babu, and L. Jacob, "Proportional fair resource allocation in vehicle-to-infrastructure networks for drive-thru internet applications," *Comput. Commun.*, vol. 40, pp. 33–50, Mar. 2014.

[5] G. Bianchi, "Performance analysis of the IEEE 802.11 distributed coordination function," *IEEE J. Sel. Areas Commun.*, vol. 18, no. 3, pp. 535–547, Mar. 2000.

[6] A. Šljivo, D. Kerkhove, L. Tian, J. Famaey, A. Munteanu, I. Moerman, J. Hoebeke, and E. D. Poorter, "Performance evaluation of IEEE 802.11ah networks with high-throughput bidirectional traffic," *Sensors*, vol. 18, no. 2, p. 325, 2018.

[7] *IEEE Standard for Information Technology—Telecommunications and Information Exchange Between Systems—Local and Metropolitan Area Networks—Specific Requirements—Part 11: Wireless LAN Medium Access Control (MAC) and Physical Layer (PHY) Specifications Amendment 2: Sub 1 GHz License Exempt Operation*, Standard 802.11ah-2016, IEEE, May 2017, pp. 1–594.

[8] B. S. Pavan, M. Mahesh, and V. P. Harigovindan, *IEEE 802.11ah for Internet Vehicles: Design Issues Challenges*. Cham, Switzerland: Springer, 2021, pp. 41–61.

[9] F. Tramarin, S. Vitturi, and M. Luvisotto, "A dynamic rate selection algorithm for IEEE 802.11 industrial wireless LAN," *IEEE Trans. Ind. Informat.*, vol. 13, no. 2, pp. 846–855, Apr. 2017.

[10] E. Khorov, A. Lyakhov, A. Krotov, and A. Guschin, "A survey on IEEE 802.11ah: An enabling networking technology for smart cities," *Comput. Commun.*, vol. 58, pp. 53–69, Mar. 2015.

[11] L. Zheng, M. Ni, L. Cai, J. Pan, C. Ghosh, and K. Doppler, "Performance analysis of group-synchronized DCF for dense IEEE 802.11 networks," *IEEE Trans. Wireless Commun.*, vol. 13, no. 11, pp. 6180–6192, Nov. 2014.

[12] M. Heusse, F. Rousseau, G. Berger-Sabbatel, and A. Duda, "Performance anomaly of 802.11b," in *Proc. IEEE INFOCOM*, vol. 2, Mar. 2003, pp. 836–843.

[13] M. Mahesh and V. P. Harigovindan, "Restricted access window-based novel service differentiation scheme for group-synchronized DCF," *IEEE Commun. Lett.*, vol. 23, no. 5, pp. 900–903, May 2019.

[14] H. Wang and A. O. Fapojuwo, "A survey of enabling technologies of low power and long range machine-to-machine communications," *IEEE Commun. Surveys Tuts.*, vol. 19, no. 4, pp. 2621–2639, 4th Quart., 2017.

[15] S. Aust, R. V. Prasad, and I. G. M. M. Niemegeers, "Outdoor long-range WLANs: A lesson for IEEE 802.11ah," *IEEE Commun. Surveys Tuts.*, vol. 17, no. 3, pp. 1761–1775, 3rd Quart., 2015.

[16] Y. Yang and S. Roy, "Grouping-based MAC protocols for EV charging data transmission in smart metering network," *IEEE J. Sel. Areas Commun.*, vol. 32, no. 7, pp. 1328–1343, Jul. 2014.

[17] N. Nawaz, M. Hafeez, S. A. R. Zaidi, D. C. Mclernon, and M. Ghogho, "Throughput enhancement of restricted access window for uniform grouping scheme in IEEE 802.11ah," in *Proc. IEEE Int. Conf. Commun. (ICC)*, May 2017, pp. 1–7.

[18] S. M. Soares and M. M. Carvalho, "Throughput analytical modeling of IEEE 802.11ah wireless networks," in *Proc. 16th IEEE Annu. Consum. Commun. Netw. Conf. (CCNC)*, Jan. 2019, pp. 1–4.

[19] A. J. Gopinath and B. Nithya, "Mathematical and simulation analysis of contention resolution mechanism for IEEE 802.11ah networks," *Comput. Commun.*, vol. 124, pp. 87–100, Jun. 2018.

[20] U. Sangeetha and A. Babu, "Performance analysis of IEEE 802.11ah wireless local area network under the restricted access window-based mechanism," *Int. J. Commun. Syst.*, vol. 32, no. 4, p. e3888, Mar. 2019.

[21] E. Khorov, A. Krotov, A. Lyakhov, R. Yusupov, M. Condoluci, M. Dohler, and I. Akyildiz, "Enabling the Internet of Things with Wi-Fi halow—Performance evaluation of the restricted access window," *IEEE Access*, vol. 7, pp. 127402–127415, 2019.

[22] Z. Ali, J. Misic, and V. B. Misic, "Performance evaluation of heterogeneous IoT nodes with differentiated QoS in IEEE 802.11ah raw mechanism," *IEEE Trans. Veh. Technol.*, vol. 68, no. 4, pp. 3905–3918, Apr. 2019.

[23] N. Ahmed, D. De, and M. I. Hussain, "A QoS-aware MAC protocol for IEEE 802.11ah-based Internet of Things," in *Proc. 15th Int. Conf. Wireless Opt. Commun. Netw. (WOCN)*, Feb. 2018, pp. 1–5.

[24] C. Kai, J. Zhang, X. Zhang, and W. Huang, "Energy-efficient sensor grouping for IEEE 802.11ah networks with max-min fairness guarantees," *IEEE Access*, vol. 7, pp. 102284–102294, 2019.

[25] O. Raeesi, J. Pirskanen, A. Hazmi, J. Talvitie, and M. Valkama, "Performance enhancement and evaluation of IEEE 802.11 ah multi-access point network using restricted access window mechanism," in *Proc. IEEE Int. Conf. Distrib. Comput. Sensor Syst.*, May 2014, pp. 287–293.

[26] N. Ahmed and M. I. Hussain, "Periodic traffic scheduling for IEEE 802.11ah networks," *IEEE Commun. Lett.*, vol. 24, no. 7, pp. 1510–1513, Jul. 2020.

[27] Q. T. Ngo, D. N. M. Dang, and Q. Le-Trung, "Extreme power saving directional MAC protocol in IEEE 802.11ah networks," *IET Netw.*, vol. 9, no. 4, pp. 180–188, Jul. 2020.

[28] J. Lei, J. Tao, J. Huang, and Y. Xia, "A differentiated reservation MAC protocol for achieving fairness and efficiency in multi-rate IEEE 802.11 WLANs," *IEEE Access*, vol. 7, pp. 12133–12145, 2019.

[29] M. Laddomada, F. Mesiti, M. Mondin, and F. Daneshgaran, "On the throughput performance of multirate IEEE 802.11 networks with variable-loaded stations: Analysis, modeling, and a novel proportional fairness criterion," *IEEE Trans. Wireless Commun.*, vol. 9, no. 5, pp. 1594–1607, May 2010.
[30] D.-Y. Yang, T.-J. Lee, K. Jang, J. B. Chang, and S. Choi, "Performance enhancement of multirate IEEE 802.11 WLANs with geographically scattered stations," *IEEE Trans. Mobile Comput.*, vol. 5, no. 7, pp. 906–919, Jul. 2006.
[31] M. A. Yazici and N. Akar, "Running multiple instances of the distributed coordination function for air-time fairness in multi-rate WLANs," *IEEE Trans. Commun.*, vol. 61, no. 12, pp. 5067–5076, Dec. 2013.
[32] U. Sangeetha and A. V. Babu, "Fair and efficient resource allocation in IEEE 802.11ah WLAN with heterogeneous data rates," *Comput. Commun.*, vol. 151, pp. 154–164, Feb. 2020.
[33] M. Mahesh, B. S. Pavan, and V. P. Harigovindan, "Data rate-based grouping to resolve performance anomaly of multi-rate IEEE 802.11ah IoT networks," *IEEE Netw. Lett.*, vol. 2, no. 4, pp. 166–170, Dec. 2020.
[34] F. Daneshgaran, M. Laddomada, F. Mesiti, and M. Mondin, "Unsaturated throughput analysis of IEEE 802.11 in presence of non ideal transmission channel and capture effects," *IEEE Trans. Wireless Commun.*, vol. 7, no. 4, pp. 1276–1286, Apr. 2008.
[35] E. Kocan, B. Domazetovic, and M. Pejanovic-Djurisic, "Range extension in IEEE 802.11ah systems through relaying," *Wireless Pers. Commun.*, vol. 97, no. 2, pp. 1889–1910, May 2017.
[36] W. Kuo, "Energy efficiency modelling for IEEE 802.11a distribution coordination function system without finite retry limits," *IET Commun.*, vol. 1, no. 2, pp. 165–172, Apr. 2007.
[37] M. Mahesh and V. P. Harigovindan, "Fuzzy based optimal and traffic-aware restricted access window mechanism for dense IoT networks," *J. Intell. Fuzzy Syst.*, vol. 37, no. 6, pp. 7851–7864, Dec. 2019.
[38] L. Tian, A. Šljivo, S. Santi, E. De Poorter, J. Hoebeke, and J. Famaey, "Extension of the IEEE 802.11ah Ns-3 simulation module," in *Proc. 10th Workshop*, New York, NY, USA, 2018, pp. 53–60.

SRI PAVAN BADARLA (Associate Member, IEEE) received the Bachelor of Technology degree in electronics and communication engineering from JNTU Hyderabad, India, and the Master of Technology degree (First class with Distinction) in digital communication engineering from Visvesvaraya Technological University, Belagavi, Karnataka, India. He is currently pursuing the Ph.D. degree with the Department of Electronics and Communication Engineering, National Institute of Technology Puducherry, Karaikal, Puducherry, India. His research interests include in the areas of wireless networks, wireless communications, the Internet of Things, IEEE 802.11 MAC layer mechanisms, and IEEE 802.11 multi-rate WLANs.

V. P. HARIGOVINDAN (Senior Member, IEEE) received the Bachelor of Technology degree in electronics and communication engineering from the University of Calicut, the Master of Technology degree in digital electronics and communication systems from Visvesvaraya Technological University with First Rank, and the Ph.D. degree from the National Institute of Technology Calicut, in 2013. He is currently an Assistant Professor with the Department of Electronics and Communication Engineering and the Associate Dean (Faculty Welfare) with the National Institute of Technology Puducherry (under Ministry of Education, Government of India). He has more than 40 international publications to his credit. Currently, he is serving as the Principal Investigator of three funded projects each from the Department of Science and Technology, Government of India, the Science and Engineering Research Board, and Microsoft AI for Earth. His research interests include in the areas of wireless networks and wireless communications.